Spectroscopic Insights into Carbon Dot Systems

Marcello Righetto [†], Alberto Privitera[†], Ilaria Fortunati[†], Dario Mosconi[†], Mirco Zerbetto[†], M. Lucia Curri[‡], Michela Corricelli[‡], Alessandro Moretto[†], Stefano Agnoli [†], Lorenzo Franco[†], Renato Bozio[†], Camilla Ferrante[†]*

[†]Department of Chemical Science and U.R. INSTM, University of Padova, Via Marzolo 1, I-35131 Padova, Italy

[‡]CNR-IPCF-Bari Division, c/o Chemistry Department, University of Bari Aldo Moro, Via Orabona 4, I-70126 Bari, Italy

Email: camilla.ferrante@unipd.it

ABSTRACT

The controversial nature of Carbon Dots (CDs) fluorescent properties, either ascribed to surface states or to small molecules adsorbed onto the carbon nanostructures, is a withstanding issue. To date, an accurate picture of CDs and an exhaustive structure-property correlation are still lacking. Using unconventional spectroscopic techniques: fluorescence correlation spectroscopy (FCS) and time-resolved electron paramagnetic resonance (TREPR), we contribute to fill this gap. Albeit electron micrographs evidence the presence of carbon cores, FCS reveals that the emission properties of CDs are based neither on those cores nor on molecular species linked to them, but rather on free molecules. TREPR provides deeper insights into the structure of carbon cores, where C-sp^2 domains are embedded within C-sp^3 scaffolds. FCS and TREPR prove to be powerful techniques, characterizing CDs as inherently heterogeneous systems, providing insights into the nature of such systems and paving the way to standardization of these nanomaterials.

KEYWORDS Carbon Dots, FCS, EPR spectroscopy, Fluorescence, Optical properties, Triplet states.

GRAPHICAL TOC

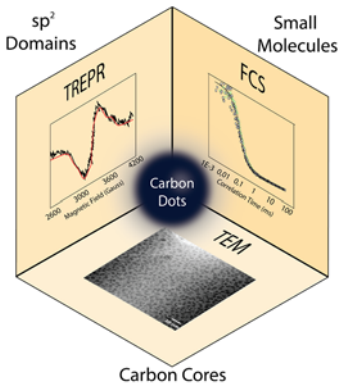

Since its inception, the fascinating idea of new carbon allotropes inspired the research on carbon-based materials beyond fullerenes [1], nanotubes [2], nanodiamonds [3], graphene [4], and yielded astounding results: nowadays, applications widely range from photovoltaics [5-7] to electrochemistry [8, 9] and biosensing[10, 11].

The opportunity to obtain environmental-friendly and biocompatible substitutes for high-performance inorganic nanostructures lies at the heart of the more recent and ever-increasing interest in carbon nano-materials. The last five years have witnessed an exponential growth in the research related to the synthesis and characterization of graphene and carbon quantum dots [12, 13]. In analogy with their inorganic counterparts, different applications are being envisaged and tested for these materials ranging from two-photon tissue imaging[14, 15] to metal ion sensing [16, 17] and catalysis [18, 19]. Furthermore, the possibility to tune the bandgap of these materials by quantum size effect [20-22] is extremely appealing for photovoltaic applications.

Looking at the inorganic counterpart, semiconductor colloidal quantum dots (QDs) offer superior and tunable opto-electronic properties [23]. However, toxicity issues hamper their use in biomedical applications and cast doubts on their large-scale production [24].

It is important to bear in mind that the successful evolution of QDs, since their inception some 25 years ago, was fueled by a fruitful synergy between a thorough characterization of their properties and the consequent development of tailored nano-structures[25, 26]. A lack of such synergy is still present in the development of carbon nano-materials and in particular of the very promising nitrogen-doped carbon dots (N-CDs). The possible underlying cause is the variable and poly-disperse nature of these nanostructures[21, 27, 28], i.e. the wide variability of structure, composition and size of the reported systems. This ill-defined nature deprives photo-physical considerations on these materials of a general significance, necessary for a rational development of their design. Many bottom-up syntheses of CDs have been proposed without reaching a complete characterization of their structural and chemical properties [29,30], further complicating this picture.

The ongoing debate on the origin of their photoluminescence is just an example of how a thorough picture for these systems is still missing [31-35,53,55]. A "multi-chromophoric scaffold" architecture is widely used as a model to account for the optical properties of many CDs [33,34,36,53,55]. This model associates the absorption features to a core state, whereas emission is ascribed to the presence of many different surface states. Within this model, excitation-dependent emission is attributed to exciton self-trapping in aromatic network or to surface chemical moieties. However, another model explains CDs properties by considering that the synthesis generates CDs with a wide dimensional distribution [37]. To a general extent, a unanimous agreement in the scientific community is still lacking.

Citric acid based N-CDs, proposed first by Sun et al.[38], were obtained through reaction between citric acid and ethylenediamine in autoclave. Resulting N-CDs displayed a high quantum yield, up to 94%. These well-performing materials, generally considered to be carbonaceous nanoparticles, were employed in a number of applications ranging from bio-imaging [39] to light-emitting devices [40,41]. During the last two years, few works demonstrated the molecular nature of the emitting species in citric-acid based N-CDs [42, 43]. Namely, albeit carbonaceous core were actually synthesized, the PL origin was univocally attributed to organic small molecules and in particular to imidazo[1,2-a]pyridine-7-carboxylic acid, 1,2,3,5-tetrahydro-5-oxo, (IPCA). This discovery casts doubts both on the "multi-chromophoric scaffold model" and on the relation between photoluminescence and carbon cores. However, the hypothesis of IPCA molecules embedded in- or connected to- the carbonaceous scaffold (i.e. multi-chromophoric scaffold model) would encompass the formation of IPCA and the presence of highly luminescent CDs.

To our view, it is of paramount importance to understand whether free small molecules effectively drive CDs samples fluorescence, because every bottom-up synthesized CDs potentially can present the same issue. The identification and separation of fluorescent molecules from carbonaceous cores via chemical methods is a tough hurdle to overcome due to the similar solubility of molecules and carbon cores [35, 42, 44, 45].

Aim of this paper is to provide a spectroscopic approach to this point and to suggest the use of less-conventional techniques, beyond basic characterization, to shed light on some missing information concerning CDs characterization. By combining optical and magnetic spectroscopies with electron micrographs, we obtain a better description of these materials and we highlight possible pitfalls of conventional characterization.

The method of choice to identify the dimension of the emitting species is Fluorescence Correlation Spectroscopy (FCS), whereas we employ Transient Electron Paramagnetic Resonance (TR-EPR) to gain information related to the photophysics of carbon cores, within the same N-CD mixture. In the following, we will discuss the results for two samples: citric acid-based N-CDs (Cit-CDs) and arginine-based N-CDs (Arg-CDs). Through investigation on Arg-CDs, we aim to extend the outreach of our considerations to other samples belonging to the CDs family. Details on their synthesis and basic characterization can be found in a previous paper [48].

We synthetized citric acid-based N-CDs (Cit-CDs) by a microwave-assisted modification of previously reported synthesis[38, 47]. The as-synthesized samples are purified by dialysis (details on synthesis can be found in SI). TEM micrograph for Cit-CDs (Fig.1A) reveals a distribution of rather uniform and spherical shaped particles. The particle size distribution, obtained by statistical analysis over 180 nanoparticles gives an average diameter 2.6±0.6 nm, similar to that of Arg-CDs (Fig. SI_3) [48]. Basic structural characterization of Cit-CDs (Figure 1) is in agreement with many literature reports on N-CDs. Raman spectrum (Fig.1B) reveals the presence of graphitic carbon (G bands) as well as oxidized carbon (D*,D',D'')[46]. Photoemission spectroscopy (XPS) further confirms this result (Fig.1C). Furthermore, the analysis of N*1s* peak ((Fig. S_1D) allows identifying the presence of pyrrolic and pyridinic nitrogen, as well as graphitic nitrogen (further discussion in SI), confirming results on Arg-CDs reported in previous papers [48].

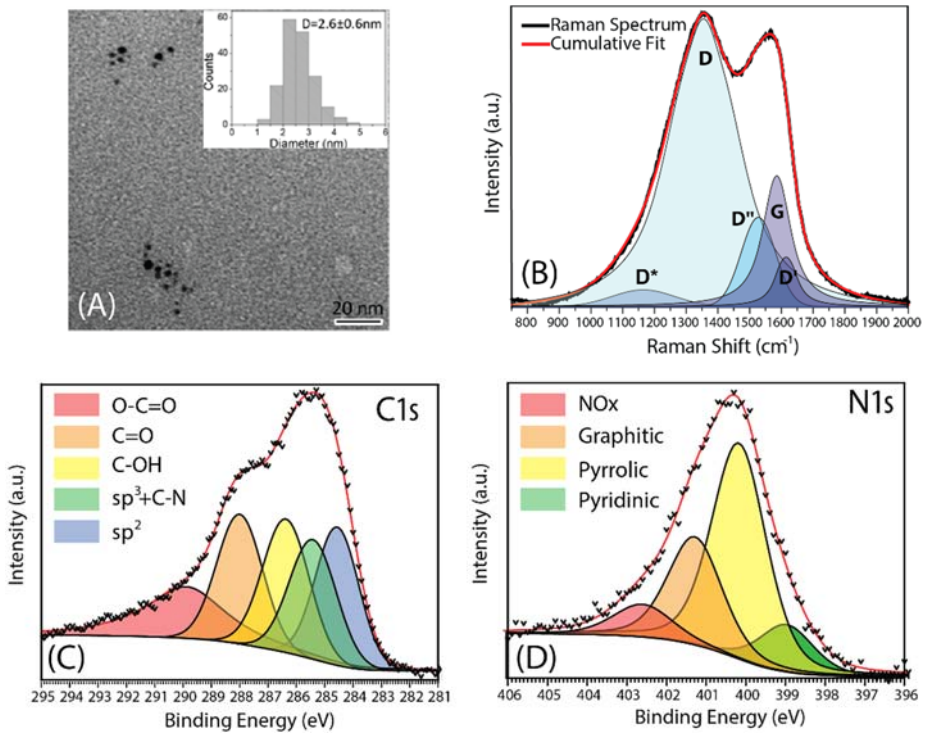

Figure 1- (A) TEM micrograph of Cit-CDs. Size distribution bar chart is shown in the inset. (B) Raman spectrum of Cit-CDs (black) and multi-peak fit (red), according to Ref. 46 (C),(D) Carbon peak and nitrogen peak of the XPS spectrum of Cit-CDs.

Therefore, standard characterization outlines for both samples typical carbon dot systems, but a direct structure-property correlation can be misleading since it does not fully uncover the possible heterogeneous nature of the sample, meaning the possibility to have both nanometer size carbonaceous nanoparticles as well as small organic molecules.

Optical properties as well are consistent with those reported in the literature [32, 35, 38] for both Cit-CDs and Arg-CDs (Fig. 2). Cit-CDs display a well-defined (30nm FWHM) absorption peak at 355nm (Fig.2A), while Arg-CDs show a broad absorption spectrum (Fig.2A). Emission wavelength dependence is reported in Fig.2B and Fig.2D for both studied samples.

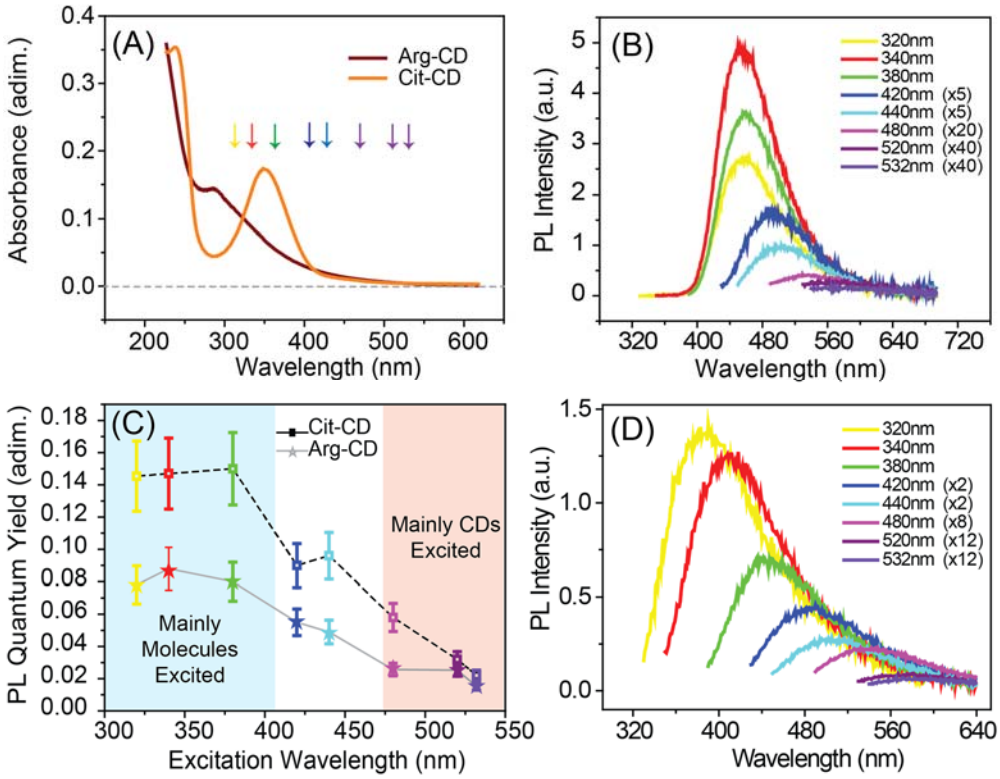

Figure 2- (A) Absorption spectrum of Cit-CDs (orange) and Arg-CDs (dark red) in water solution. Colored arrows indicate excitation wavelengths, color coding is respected and is related to excitation wavelength used for emission measurements. (B) Excitation wavelength dependence of Cit-CDs emission. (C) Excitation wavelength dependence of PL QY for Cit-CDs and Arg-CDs. Blue and red shadowed regions identify the leading contribution of different species (molecular species and CDs). (D) Excitation wavelength dependence of Arg-CDs emission.

Excitation energy dependent properties are a puzzling question related to the wider topic of CDs photoluminescence mechanism. Albeit complete agreement on the origin of this phenomenon is still lacking, excitation-energy dependent emission is considered distinctive of CDs systems. Possible explanations range from heterogeneity in sample composition to slow solvent relaxation properties [32, 34, 35]. Recent work employing single molecule and anisotropy measurements revealed the presence of different emitters within CDs emission band. [34,53] According to these papers, the progressive red-shift of the emission band as the excitation wavelength is also tuned towards the red

(Fig. 2B and 2D) originates from the presence of different moieties/entities (for example aggregates of specific moieties) characterized by an overlapping spectral distribution. When the excitation wavelength is changed, different moieties/entities are excited to a different extent. In these works, the authors still maintain that these entities are either embedded within the sp^3 carbon core of the CDs or attached to its surface.

On the other hand, Yang demonstrated that a citrazinic acid derivative called IPCA is responsible for the main optical properties of citric-acid based N-CDs [42, 43]. Within this framework, optical properties of Cit-CDs should combine those of IPCA with the one of carbon cores.

Photoluminescence quantum yield (QY) is the ratio between the number of emitted and absorbed photons, and is usually constant for a single emitting state/moiety. Instead, we observed excitation energy dependence of QY, for both studied samples. In both Cit-CDs and Arg-CDs we observe QY to be almost stable, when sweeping the excitation wavelength from 320nm to 380nm (Fig.2C). Yet QY rapidly decreases above 440nm excitation. Albeit similar behavior in QDs was ascribed to hot-exciton trapping [54], we suggest it to stem from the heterogeneous composition of CDs solutions (i.e. in as-synthesized CDs both free molecules and nanometric sized carbon particles are present). One photon absorption is shared between molecular and carbon core species, whereas their emission efficiencies are different [43]. For instance, in Cit-CDs 520nm photons are not expected to excite IPCA molecules and the resulting emission is assigned to carbon cores. [42,43] Similar results were recently reported by Rogach, for Cit-CDs.[55] Noteworthy, the QY behavior of Arg-CDs is akin to that of Cit-CDs. (A more thorough discussion on Arg-CDs solution composition is given in SI)

We took advantage of Fluorescence Correlation Spectroscopy (FCS) in order to confirm the pivotal role played by free IPCA molecule in Cit-CDs and also to evaluate the origin of fluorescence in the Arg-CDs systems.

FCS records fluorescence intensity fluctuations in femtoliter volumes [49]. A wide variety of processes concur to these fluctuations and potentially give rise to structured curves at different time

scale. Among these, a pivotal role is played by translational diffusion of the luminescent species inside the investigated volume [50]. We analyze the CDs fluorescence autocorrelation curve to estimate the diffusion coefficient of the emitting species and, from this, its average hydrodynamic size. FCS curves for Arg-CDs and Cit-CDs (Fig.3) are typical of molecular entities and very similar to the curve collected for the reference standard (Coumarin 503), whose chemical formula is given in SI (curves are normalized to allow direct comparison).

FCS curves of Arg-CDs and Cit-CDs are fitted to the equation

$$G(\tau) = \frac{1}{N}\left(1+\frac{\tau}{\tau_D}\right)^{-1}\left(1+\frac{\tau}{S^2\tau_D}\right)^{-1/2}, \qquad (1)$$

Where N is the number of molecule in focal volume and the characteristic time τ_D is associated with the diffusion coefficient D via relation $\tau_D = \omega_0^2/4D$. S is the confocal shape factor, i.e. the ratio between axial (z_0) and lateral (ω_0) radius at which intensity is reduced by e^{-2} factor. In normalized FCS curves, N is set equal to 1. This model accounts for fluorescence intensity fluctuation caused by translational diffusion of fluorophores, and well fits recorded curves (Fig.3). Coumarin 503 is used as standard to determine the parameters ω_0 and z_0, which in turn are used to obtain the hydrodynamic radius of CDs via Stokes-Einstein relation

$$R_H = \frac{4k_B T\tau_D}{6\pi\eta\omega_0^2}. \qquad (2)$$

Where k_B is the Boltzmann constant, T is the laboratory absolute temperature, τ_D is the CD diffusion time gained from fitting, and η is the solution viscosity.

FCS fitting outcomes reveal an average hydrodynamic radius of $R_H = 4.9 \pm 0.8$ Å for Cit-CDs and $R_H = 5.4 \pm 0.7$ Å for Arg-CDs (for details, see SI). These dimensions are typical of common organic dyes. Notably, these estimates are also in agreement with the one of the IPCA molecule found by Yang in Cit-CDs [42]. Consequently, we can unequivocally state that Arg-CDs and Cit-CDs

emission properties when excited in the 370-440 nm range are dominated by a “molecular” entity with below-nm hydrodynamic radius.

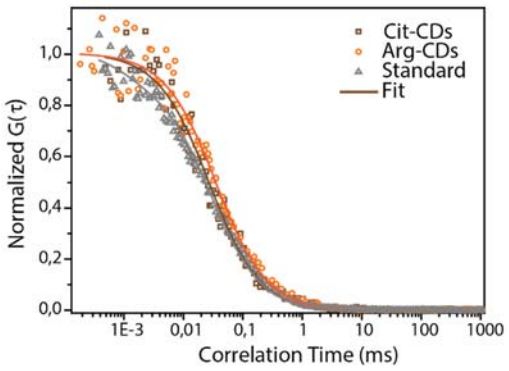

Figure 3- Normalized FCS curves for Cit-CDs (brown dots), Arg-CDs (orange dots), and Coumarin 153 (grey dots). Normalization allows direct comparison between diffusional times, fitting was performed before normalization operation. FCS curves are fitted (solid lines) to the translational diffusion model in Eq.1

Notably, FCS measurements performed at different excitation wavelength (370nm, 400nm, 440nm, throughout the red region in Fig.2C) are very similar. We stress the fact that FCS results refer to translational diffusion of emitting species. Therefore, emission under reported excitation wavelengths is originated by free molecular species, having comparable diffusion coefficients.

FCS curves measured under 488nm excitation bolstered our interpretation of CDs heterogeneity. We observe larger hydrodynamics radii at this excitation wavelength for both samples (Fig. SI_10). This observation is consistent with both the dimensions of CDs found in TEM and the low QY reported in Fig. 2C, and suggests that emission at these excitation wavelengths is dominated by poorly emitting carbonaceous cores. A detailed discussion on excitation wavelength resolved FCS is carried out in SI.

With the aim to investigate the carbon cores structure and their photophysics, we employed TREPR technique with microsecond time resolution. Being selective and sensitive to paramagnetic

species that are generated by photoexcitation, TREPR technique allows us probing the excited state dynamics of those species that cannot be investigated using photoluminescence measurements. [48]

The TREPR spectra (Fig. 4A and SI_11) of our samples show broad bands (about 100 mT) with an emissive/absorptive character and a decay time of about 20 µs, all features typical of photoexcited triplet states.[51]

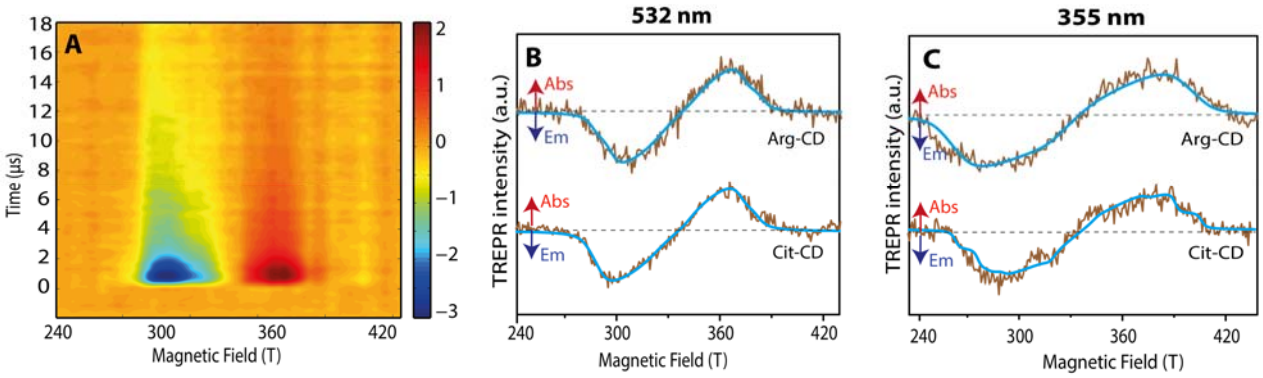

Figure 4– (A) Two-dimensional TREPR spectrum of Cit-CD acquired after 532 nm laser pulse. (B, C) One-dimensional TREPR spectra taken at 1µs after a 532 nm or 355 nm laser pulse of Arg-CD and Cit-CD (brown lines) and best fit spectral simulations (blue lines). The measurements were performed at 130K. Abs = Absorption, Em = Emission.

The generation of excited triplet states is a process competitive with the emission from excited singlet. The detection of triplet states therefore is to be attributed to some non-fluorescent components in the CDs samples. From best-fit spectral simulation of TREPR acquired using 532 nm radiation (Fig. 4B), we obtain the Zero Field Splitting (ZFS) parameters D and E, defining the magnetic dipolar interaction between the two electrons of the triplet state. The D parameter is related to the mean distance between the two unpaired electrons, whereas the E parameter defines the deviation from axial symmetry of the triplet state wavefunction. Simulated values are D=1380MHz for both CDs and E=250MHz and 310MHz, for Arg-CDs and Cit-CDs, respectively.

In order to have a hint of the spatial delocalization of the carbon cores triplet wavefunctions, it can be useful to compare their D values with those of some aromatic or hetero-aromatic species. This comparison suggests that CDs excited triplet state is delocalized on molecular structures

composed of approximately 4-5 aromatic rings.[52] These dimensions are not compatible with the hydrodynamic radii estimated by FCS in 370-440nm excitation interval. Therefore, TREPR further demonstrates the presence of different entities within CDs solutions. The estimated delocalization of the triplet wavefunction on sp^2 domains suggest the presence of aromatic domains within cores of dimensions larger than about 2 nm, as measured by TEM and by FCS at 488nm excitation. The identification of aromatic fragments within the CD is in agreement with the description of CDs carbon cores suggested by Feldmann [33] who demonstrated the presence of polyaromatic hydrocarbon (PAH) domains embedded in a sp^3-hybridized carbon matrix. The large inhomogeneous broadening observed in TREPR spectra is a possible consequence of the size and local environment heterogeneity of aromatic domains.

Further insight on the photo-physics and the structure of the carbon cores is provided by TREPR measurements using 355 nm excitation (Fig. 4C). TREPR spectra of both samples show a photoexcited triplet signal much broader than those observed using visible photoexcitation (Fig. 4B). The simulation yields D and E values (D= 2100 and 1900 MHz, E=500 and 400 MHz respectively for Arg-CDs and Cit-CDs) compatible with aromatic domains composed of smaller aromatic units extending for about three condensed aromatic rings.[52] This is again compatible with the results of Feldmann[33] and indicates that using different excitation wavelengths, different aromatic domains are excited.

Considering the complete picture emerging from our observations, small photo-luminescent molecules free in solution are mainly responsible for the emissive properties of CDs systems, in 320-450nm excitation range. On the other hand, excitation above 480nm allows observing almost selectively carbon cores. These photophysical entities display lower QYs and bulkier hydrodynamics radii, consistently with TEM micrographs results. Moreover, by TREPR we delve into their structure: aromatic domains embedded within the carbon cores are responsible for the generation of long-living excited triplet states. The presence of such triplets is consistent with recorded low QY.

The combination of optical and magnetic spectroscopies reveals the complex nature of the system, made up of different species, presenting non-homogeneous photo-physics. In agreement with recently reported PL anisotropy measurements [34], different emitters concur to the puzzling and unusual emission of CDs.

In conclusion, FCS and TREPR showed that the CDs systems synthesized by us behave as a multiple facet entities, often switching through the borders separating single molecules and nanomaterials. According to this picture, for our CDs we could devise applications in catalysis or photodynamic therapy. Their use as fluorescent tracers must take into account that luminescence mainly originates from free small molecules dispersed in solution: consequently, those molecules, rather than carbon cores, will label biological substrates.

The outreach of our results is inherently limited to the samples investigated in this work, i.e. microwave assisted one-pot CDs synthesis. Nevertheless, the resemblance of optical and structural properties suggests a potential extension of these results to CDs from different synthetic routes. Further experimental work is currently underway to test this hypothesis. Dealing with this complexity, we want to remark how FCS and TREPR, two unconventional techniques, can lend a precious hand to investigate the properties of pristine and chemically functionalized CDs.

ACKNOWLEDGMENT

The authors acknowledge MIUR (PRIN Prot.N. 2012T9XHH7) and University of Padova (PRAT Prot. N. CPDA155454) for financial support. I.F. acknowledges the granting of “Assegno di Ricerca Senior” (Repertorio 156-2014) by the University of Padova.

Supporting information Available. Structural characterization of CDs. pH resolved characterization of Cit-CDs. Detail on experimental methods and discussion on FCS and TREPR characterization. This information are available free of charge *via* the Internet at http://pubs.acs.org.

REFERENCES

1. Kroto, H. W.; Heath, J. R.; O'Brien, S. C.; Curl, R. F.; Smalley, R. E. C60: Buckminsterfullerene. *Nature* **1985**, 318, 162-163.

2. Tasis, D.; Tagmatarchis, N.; Bianco, A.; Prato, M. Chemistry of Carbon Nanotubes. *Chem. Rev.* **2006**, 106, 1105-1136.

3. Mochalin, V. N.; Shenderova, O.; Ho, D.; Gogotsi, Y. The Properties and Applications of Nanodiamonds. *Nat. Nano.* **2012**, 7, 11-23.

4. Geim, A. K.; Novoselov, K. S. The Rise of Graphene. *Nat. Mater.* **2007**, 6, 183-191.

5. Bernardi, M.; Lohrman, J.; Kumar, P. V.; Kirkeminde, A.; Ferralis, N.; Grossman, J. C.; Ren, S. Nanocarbon-Based Photovoltaics. *ACS Nano* **2012**, 6, 8896-8903.

6. Martín, N. Carbon Nanoforms for Photovoltaics: Myth or Reality? *Adv. En. Mat.* **2016**, 1601102-n/a.

7. Gong, M.; Shastry, T. A.; Xie, Y.; Bernardi, M.; Jasion, D.; Luck, K. A.; Marks, T. J.; Grossman, J. C.; Ren, S.; Hersam, M. C. Polychiral Semiconducting Carbon Nanotube–Fullerene Solar Cells. *Nano Lett.* **2014**, 14, 5308-5314.

8. Frackowiak, E.; Béguin, F. Carbon Materials for the Electrochemical Storage of Energy in Capacitors. *Carbon* **2001**, 39, 937-950.

9. Ambrosi, A.; Chua, C. K.; Bonanni, A.; Pumera, M. Electrochemistry of Graphene and Related Materials. *Chem. Rev.* **2014**, 114, 7150-7188.

10. Hsiao, W. W.-W.; Hui, Y. Y.; Tsai, P.-C.; Chang, H.-C. Fluorescent Nanodiamond: A Versatile Tool for Long-Term Cell Tracking, Super-Resolution Imaging, and Nanoscale Temperature Sensing. *Acc. Chem. Res* **2016**, 49, 400-407.

11. Yang, N.; Chen, X.; Ren, T.; Zhang, P.; Yang, D. Carbon Nanotube Based Biosensors. *Sensors and Actuators B: Chemical* **2015**, 207, 690-715.

12. Ritter, K. A.; Lyding, J. W. The Influence of Edge Structure on the Electronic Properties of Graphene Quantum Dots and Nanoribbons. *Nat. Mater.* **2009**, 8, 235-242.

13. Li, H.; Kang, Z.; Liu, Y.; Lee, S.-T. Carbon Nanodots: Synthesis, Properties and Applications. *J. Mater. Chem.* **2012**, 22, 24230-24253.

14. Liu, Q.; Guo, B.; Rao, Z.; Zhang, B.; Gong, J. R. Strong Two-Photon-Induced Fluorescence from Photostable, Biocompatible Nitrogen-Doped Graphene Quantum Dots for Cellular and Deep-Tissue Imaging. *Nano Lett.* **2013**, 13, 2436-2441.

15. Zhu, S.; Zhang, J.; Qiao, C.; Tang, S.; Li, Y.; Yuan, W.; Li, B.; Tian, L.; Liu, F.; Hu, R. et al. Strongly Green-Photoluminescent Graphene Quantum Dots for Bioimaging Applications. *Chem. Comm.* **2011**, 47, 6858-6860.

16. Dong, Y.; Shao, J.; Chen, C.; Li, H.; Wang, R.; Chi, Y.; Lin, X.; Chen, G. Blue Luminescent Graphene Quantum Dots and Graphene Oxide Prepared by Tuning the Carbonization Degree of Citric Acid. *Carbon* **2012**, 50, 4738-4743.

17. Wang, Y.; Hu, A. Carbon Quantum Dots: Synthesis, Properties and Applications. *J. Mater. Chem. C* **2014**, 2, 6921-6939.

18. Favaro, M.; Ferrighi, L.; Fazio, G.; Colazzo, L.; Di Valentin, C.; Durante, C.; Sedona, F.; Gennaro, A.; Agnoli, S.; Granozzi, G. Single and Multiple Doping in Graphene Quantum Dots: Unraveling the Origin of Selectivity in the Oxygen Reduction Reaction. *ACS Catalysis* **2015**, 5, 129-144.

19. Fei, H.; Ye, R.; Ye, G.; Gong, Y.; Peng, Z.; Fan, X.; Samuel, E. L. G.; Ajayan, P. M.; Tour, J. M. Boron- and Nitrogen-Doped Graphene Quantum Dots/Graphene Hybrid Nanoplatelets as Efficient Electrocatalysts for Oxygen Reduction. *ACS Nano* **2014**, 8, 10837-10843.

20. Kim, S.; Hwang, S. W.; Kim, M.-K.; Shin, D. Y.; Shin, D. H.; Kim, C. O.; Yang, S. B.; Park, J. H.; Hwang, E.; Choi, S.-H.; Ko, G. et al. Anomalous Behaviors of Visible Luminescence from Graphene Quantum Dots: Interplay between Size and Shape. *ACS Nano* **2012**, 6, 8203-8208..

21. Cao, L.; Meziani, M. J.; Sahu, S.; Sun, Y.-P. Photoluminescence Properties of Graphene Versus Other Carbon Nanomaterials. *Acc. Chem. Res.* **2013**, 46, 171-180.

22. Fuyuno, N.; Kozawa, D.; Miyauchi, Y.; Mouri, S.; Kitaura, R.; Shinohara, H.; Yasuda, T.; Komatsu, N.; Matsuda, K. Drastic Change in Photoluminescence Properties of Graphene Quantum Dots by Chromatographic Separation. *Adv. Opt. Mat.* **2014**, 2, 983-989.

23. Saha, A.; Chellappan, K. V.; Narayan, K. S.; Ghatak, J.; Datta, R.; Viswanatha, R. Near-Unity Quantum Yield in Semiconducting Nanostructures: Structural Understanding Leading to Energy Efficient Applications *J. Phys. Chem. Lett*. **2013**, 4, 3544-3549.

24. Winnik, F. M.; Maysinger, D. Quantum Dot Cytotoxicity and Ways to Reduce It. *Acc. Chem. Res.* **2013**, 46, 672-680.

25. Kim, J. Y.; Voznyy, O.; Zhitomirsky, D.; Sargent, E. H. 25th Anniversary Article: Colloidal Quantum Dot Materials and Devices: A Quarter-Century of Advances. *Adv. Mat.* **2013**, 25, 4986-5010.

26. Klimov, V. I. Spectral and Dynamical Properties of Multiexcitons in Semiconductor Nanocrystals. *Ann. Rev. Phys. Chem.* **2007**, 58, 635-673.

27. Baker, S. N.; Baker, G. A. Luminescent Carbon Nanodots: Emergent Nanolights. *Angew. Chem. Int. Ed.* **2010**, 49, 6726-6744.

28. Zhang, Z.; Zhang, J.; Chen, N.; Qu, L. Graphene Quantum Dots: An Emerging Material for Energy-Related Applications and Beyond. *En. & Env. Sc.* **2012**, 5, 8869-8890.

29. Zhang, Z.; Sun, W.; Wu, P. Highly Photoluminescent Carbon Dots Derived from Egg White: Facile and Green Synthesis, Photoluminescence Properties, and Multiple Applications. *ACS Sus. Chem. & Eng.* **2015**, 3, 1412-1418.

30. Zhang, J.; Yu, S.-H. Carbon Dots: Large-Scale Synthesis, Sensing and Bioimaging. *Mat. Today* **2016**, 19, 382-393.

31. Dekaliuk, M. O.; Viagin, O.; Malyukin, Y. V.; Demchenko, A. P. Fluorescent Carbon Nanomaterials: "Quantum Dots" or Nanoclusters? *Phys. Chem. Chem. Phys.* **2014**, 16, 16075-16084.

32. Strauss, V.; Margraf, J. T.; Dolle, C.; Butz, B.; Nacken, T. J.; Walter, J.; Bauer, W.; Peukert, W.; Spiecker, E.; Clark, T. et al. Carbon Nanodots: Toward a Comprehensive Understanding of Their Photoluminescence. *J. Am. Chem. Soc.* **2014**, 136, 17308-17316.

33. Fu, M.; Ehrat, F.; Wang, Y.; Milowska, K. Z.; Reckmeier, C.; Rogach, A. L.; Stolarczyk, J. K.; Urban, A. S.; Feldmann, J. Carbon Dots: A Unique Fluorescent Cocktail of Polycyclic Aromatic Hydrocarbons. *Nano Lett.* **2015**, 15, 6030-6035.

34. Demchenko, A. P.; Dekaliuk, M. O. The Origin of Emissive States of Carbon Nanoparticles Derived from Ensemble-Averaged and Single-Molecular Studies. *Nanosc.* **2016**, 8, 14057-14069.

35. Zhu, S.; Song, Y.; Zhao, X.; Shao, J.; Zhang, J.; Yang, B. The Photoluminescence Mechanism in Carbon Dots (Graphene Quantum Dots, Carbon Nanodots, and Polymer Dots): Current State and Future Perspective. *Nano Res.* **2015**, 8, 355-381.

36. Sciortino, A.; Marino, E.; Dam, B. v.; Schall, P.; Cannas, M.; Messina, F. Solvatochromism Unravels the Emission Mechanism of Carbon Nanodots. *J. Phys. Chem. Lett.* **2016**, 7, 3419-3423.

37. Ghosh, S.; Chizhik, A. M.; Karedla, N.; Dekaliuk, M. O.; Gregor, I.; Schuhmann, H.; Seibt, M.; Bodensiek, K.; Schaap, I. A. T.; Schulz, O.; Demchenko, A. P. et al. Photoluminescence of Carbon Nanodots: Dipole Emission Centers and Electron–Phonon Coupling. *Nano Lett.* **2014**, 14, 5656-5661.

38. Qu, D.; Zheng, M.; Zhang, L.; Zhao, H.; Xie, Z.; Jing, X.; Haddad, R. E.; Fan, H.; Sun, Z. Formation Mechanism and Optimization of Highly Luminescent N-Doped Graphene Quantum Dots. *Sci. Rep.* **2014**, 4.

39. Xu, G.; Zeng, S.; Zhang, B.; Swihart, M. T.; Yong, K.-T.; Prasad, P. N. New Generation Cadmium-Free Quantum Dots for Biophotonics and Nanomedicine. *Chem. Rev.* **2016**, 116, 12234-12327.

40. Zhang, X.; Zhang, Y.; Wang, Y.; Kalytchuk, S.; Kershaw, S. V.; Wang, Y.; Wang, P.; Zhang, T.; Zhao, Y.; Zhang, H. et al. Color-Switchable Electroluminescence of Carbon Dot Light-Emitting Diodes. *ACS Nano* **2013**, 7, 11234-11241.

41. Li, X.; Zhang, S.; Kulinich, S. A.; Liu, Y.; Zeng, H. Engineering Surface States of Carbon Dots to Achieve Controllable Luminescence for Solid-Luminescent Composites and Sensitive Be^{2+} Detection. *Sci. Rep.* **2014**, 4, 4976.

42. Song, Y.; Zhu, S.; Zhang, S.; Fu, Y.; Wang, L.; Zhao, X.; Yang, B. Investigation from Chemical Structure to Photoluminescent Mechanism: A Type of Carbon Dots from the Pyrolysis of Citric Acid and an Amine. *J. Mat. Chem. C* **2015**, 3, 5976-5984.

43. Shi, L.; Yang, J. H.; Zeng, H. B.; Chen, Y. M.; Yang, S. C.; Wu, C.; Zeng, H.; Yoshihito, O.; Zhang, Q. Carbon Dots with High Fluorescence Quantum Yield: The Fluorescence Originates from Organic Fluorophores. *Nanoscale* **2016**, 8, 14374-14378.

44. Vinci, J. C.; Ferrer, I. M.; Seedhouse, S. J.; Bourdon, A. K.; Reynard, J. M.; Foster, B. A.; Bright, F. V.; Colón, L. A. Hidden Properties of Carbon Dots Revealed after Hplc Fractionation. *J. Phys. Chem. Lett.* **2013**, 4, 239-243.

45. Song, Y.; Zhu, S.; Xiang, S.; Zhao, X.; Zhang, J.; Zhang, H.; Fu, Y.; Yang, B. Investigation into the Fluorescence Quenching Behaviors and Applications of Carbon Dots. *Nanosc.* **2014**, 6, 4676-4682.

46. Claramunt, S.; Varea, A.; López-Díaz, D.; Velázquez, M. M.; Cornet, A.; Cirera, A. The Importance of Interbands on the Interpretation of the Raman Spectrum of Graphene Oxide. *J. Phys. Chem. C* **2015**, 119, 10123-10129.

47. Karfa, P.; Roy, E.; Patra, S.; Kumar, S.; Tarafdar, A.; Madhuri, R.; Sharma, P. K. Amino Acid Derived Highly Luminescent, Heteroatom-Doped Carbon Dots for Label-Free Detection of Cd2+/Fe3+, Cell Imaging and Enhanced Antibacterial Activity. *RSC Adv.* **2015**, 5, 58141-58153.

48. Mosconi, D.; Mazzier, D.; Silvestrini, S.; Privitera, A.; Marega, C.; Franco, L.; Moretto, A. Synthesis and Photochemical Applications of Processable Polymers Enclosing Photoluminescent Carbon Quantum Dots. *ACS Nano* **2015**, 9, 4156-4164.

49. Fortunati, I.; Weber, V.; Giorgetti, E.; Ferrante, C. Two-Photon Fluorescence Correlation Spectroscopy of Gold Nanoparticles under Stationary and Flow Conditions. *J. Phys. Chem. C* **2014**, 118, 24081-24090.

50. Ries, J.; Schwille, P. Fluorescence Correlation Spectroscopy. *BioEssays* **2012**, 34, 361-368.

51. Atherton, N. M., Principles of Electron Spin Resonance; Ellis Horwood, 1993.

52. Montalti, M.; Credi, A.; Prodi, L.; Gandolfi, M. T. Handbook of Photochemistry, Third Edition; CRC Press, 2006.

53. Sharma, A.; Gadly, T.; Gupta, A.; Ballal, A.; Ghosh, S. K.; Kumbhakar, M., Origin of Excitation Dependent Fluorescence in Carbon Nanodots. *J. Phys. Chem. Lett.* **2016**, 7, 3695-3702.

54. Righetto, M.; Minotto, A.; Bozio, R. Bridging Energetics and Dynamics of Exciton Trapping in Core-Shell Quantum Dots *J. Phys. Chem. C* **2017**, 121, 1,896-902.

55. Schneider, J.; Reckmeier, C. J.; Xiong, Y.; von Seckendorff, M.; Susha, A. S.; Kasák, P.; Rogach, A. L. Molecular Fluorescence in Citric Acid-Based Carbon Dots. *J. Phys. Chem C* **2017**, 121, 2014-2022.